

REFERENCE

NBS

PUBLICATIONS

NBSIR 82-2614



A11106 261523

Prediction of Floating Solid Velocities in Unsteady Partially Filled Pipe Flow

Drainage Research Group
Department of Building Technology
Brunel University
Uxbridge
Middx, U.K.

July 1983



QC

100

DEPARTMENT OF COMMERCE

.U56

NATIONAL BUREAU OF STANDARDS

82-2614

1983

NBSIR 82-2614

**THE PREDICTION OF FLOATING SOLID
VELOCITIES IN UNSTEADY PARTIALLY
FILLED PIPE FLOW**

Dr. J. A. Swaffield

Drainage Research Group
Department of Building Technology
Brunel University
Uxbridge
Middx., U.K.

July 1983

U.S. DEPARTMENT OF COMMERCE, Malcolm Baldrige, *Secretary*
NATIONAL BUREAU OF STANDARDS, Ernest Ambler, *Director*

SUMMARY

The method of characteristics is applied to solve the unsteady partially filled pipe flow equations and to predict the velocity of floating solids assumed to travel at a fixed percentage of the local flow velocity.

Experimental verification for the technique is provided for cylindrical solids in a 100 mm diameter drainage pipe at a range of gradients from 1/40 to 1/150.

The system upstream boundary conditions are shown to be capable of representation in terms of the infow energy at the pipe entry section.

Steady flow floating solid to flow velocity ratios are presented at 1/150 pipe gradient and further areas of experimental work to determine the variation of these ratios with pipe gradient and flow depth are identified.

PREFACE

This report is one of a group documenting National Bureau of Standards (NBS) research and analysis efforts in developing water conservation test methods, analysis, economics, and strategies for implementation and acceptance. This work is sponsored by the Department of Housing and Urban Development/Office of Policy Development and Research, Division of Energy Building Technology and Standards, under HUD Interagency Agreement H-48-78.

Report prepared by Dr. J. A. Swaffield, Senior Lecturer, Drainage Research Group, Department of Building Technology, Brunel University, Uxbridge, U.K., as a result of a study leave period as a guest research worker at NBS/Stevens Institute of Technology.

Experimental results included in this report are drawn from work undertaken by the Drainage Research Group at Brunel University on behalf of NBS in June 1980.

TABLE OF CONTENTS

	<u>Page</u>
SUMMARY	iii
PREFACE	iv
LIST OF FIGURES AND TABLES	vi
NOTATION	vii
1. INTRODUCTION	1
2. BASIS FOR THE TRANSPORT MODEL	2
2.1 VELOCITY PROFILES IN OPEN CHANNEL FLOW	2
2.2 FLOATING SOLID VELOCITIES	2
2.3 PREDICTION OF FLOW ATTENUATION IN PARTIALLY FILLED PIPE FLOW ...	2
2.3.1 Initial Conditions	6
2.3.2 Boundary Conditions	6
2.4 CALCULATION OF SOLID VELOCITY	9
3. DISCUSSION OF THE FLOATING SOLID TRANSPORT MODEL	12
3.1 STEADY FLOW SOLID TRANSPORT VELOCITY MEASUREMENT	12
3.2 EXPERIMENTAL VERIFICATION	12
3.3 ENTRY BOUNDARY CONDITIONS AND UNSTEADY FLOW SOLID TRANSPORT	15
3.4 FLOATING SOLID TO FLOW VELOCITY RATIO AND ITS EFFECT ON PREDICTED SOLID TRANSPORT	21
4. CONCLUSIONS AND FURTHER WORK	26
REFERENCES	27

LIST OF FIGURES AND TABLES

	<u>Page</u>
Figure 1. Typical velocity profile in open channel or partially filled pipe flow	3
Figure 2. Floating solid velocity in open channel flow	4
Figure 3. Summary of method of characteristics solution to the unsteady partially filled pipe flow equations	5
Figure 4. Development of the solution in the x-t plane	7
Figure 5. Alternative entry boundary equations	8
Figure 6. Solid migration through an inflow profile	10
Figure 7. Calculation of floating solid velocity and position in the pipe	11
Figure 8. Steady flow solid velocity results at a 1/150 pipe gradient	13
Figure 9. Schematic layout of solid transport test rig	14
Figure 10. Typical solid transport data as produced by the Apple II system	16
Figure 11. Comparison of observed and predicted solid velocities along the test pipe at a gradient of 1/40	17
Figure 12. Comparison of observed and predicted solid velocities along the test pipe at a gradient of 1/80	18
Figure 13. Comparison of observed and predicted solid velocities along the test pipe at a gradient of 1/150	19
Figure 14. Comparison of flow velocity and depth predictions at pipe entry for the normal depth and inflow energy boundary conditions	20
Figure 15. Maximum predicted depths along the test pipe and both normal flow depth and entry energy upstream boundary conditions	22
Figure 16. Illustration of the effect of solid insertion time on predicted transport along the test pipe	25
Table 1. Predicted Total Solid Transport Time for 14m Pipe Gradients and Velocity Ratios	26

NOTATION

A	Pipe flow cross section area
C^+ , C^-	Notation referring to the positive and negative characteristics
C	Chezy coefficient
c	Wave speed
D	Pipe diameter
E	Specific energy = $h + V^2/2g$
F_r	Froude $N^\circ = V/\sqrt{gh}$
G	Pipe slope
g	Acceleration due to gravity
h	Flow depth
L	Pipe length
m	Hydraulic mean depth
N,n	N° of pipe length sections employed
P	Wetted channel perimeter
Q	Flow rate
S_o	Pipe slope
S	Slope of energy grade line, defined by Manning's Equation
T	Surface width of flow within partially filled channel
t	Time
V	Local mean velocity
X1-4	Functions of h, V, c and s calculated at each base point at each time step
x	Distance, positive in initial flow direction
α	Pipe slope, $S_o = \sin\alpha$
Δt	Time step

Δx	Pipe section length
θ	$\Delta t / \Delta x$
ρ	Fluid density
τ_0	Wall to fluid shear stress

Subscripts

A, B, C	Calculated points in an x-t grid at time t
c	Critical flow conditions
n	Normal flow conditions
P	Calculated points in an x-t grid at time t + Δt
R, S, S'	Interpolated points in an x-t grid at time t
1	Upstream boundary section
N+1	Downstream boundary section

1. INTRODUCTION

The transport of waste solids under unsteady flow conditions in partially filled drainage pipes may be characterized by the specific gravity of the solid. In the case where the specific gravity of the solid, including its saturated state, exceeds unity, it is necessary to include solid to pipe wall sliding friction in the model, together with a representation of the significant flow depth change that can occur across the solid. This case was the subject of previous reports in the series (1,2).

However, if the solid specific gravity is less than unity then the solid may be considered to "float" in the flow if sufficient depth is provided by the transporting fluid. Quite obviously the attenuation effects previously described (3,4) will eventually reduce the transporting flow depth to the point where solid to pipe wall sliding friction is again established; however, this will indicate the imminence of solid deposition and, as such, may be used as a cut-off indicator for the proposed floating solid transport model.

This paper presents a mathematical model, based on the application of the method of characteristics to solve the unsteady open channel flow equations, including boundary conditions chosen to represent the flow entry energy. The model predictions are compared with experimental results based on NBS cylindrical model solid transport tests undertaken at Brunel University in 1980.

2. BASIS FOR THE TRANSPORT MODEL

2.1 VELOCITY PROFILES IN OPEN CHANNEL FLOW

Figure 1 illustrates typical fluid velocity profiles in open channel or partially filled pipe flow. These profiles are influenced by the presence of the channel walls as well as the free surface, and, in unsteady flow will vary with flow depth in circular cross-section channels.

In view of the complexity of velocity profiles across a pipe flowing partially full, and the lack of both detailed experimental data and theoretical velocity distribution expressions, similar to those available for full bore pipe flow, it is necessary to generalize the flow velocity profiles. For open channel flow in channels having circular cross-sections, it is generally accepted (5) that the maximum velocity occurs at about 15-25 percent depth below the free surface and that this free surface velocity is approximately 80-85 percent of the mean velocity, which occurs at about 60 percent depth below the free surface. These figures will change with depth-diameter ratio, roughness, etc.

2.2 FLOATING SOLID VELOCITIES

If a model solid has a specific gravity less than unity and is sufficiently small to cause little flow obstruction, it may be assumed to travel at the local flow velocity appropriate to its position on the fluid velocity profile described above. Thus, a small solid floating on, or just below, the flow free surface would be expected to move at 80 percent, or more, of the flow mean velocity, as shown in Figure 2.

In this case, a calculation technique that predicts unsteady flow local mean velocities may be simply utilized to yield both the solid velocity and a measure of its progress along any open channel.

2.3 PREDICTION OF FLOW ATTENUATION IN PARTIALLY-FILLED PIPE FLOW

The application of the method of characteristics to the prediction of flow depth, mean velocity and associated attenuating flow rate in partially filled pipe flow has been detailed previously (3) and the basic theory will not be restated here. Figure 3 illustrates the transformation of the unsteady flow equations of continuity and motion:

$$g \frac{\partial h}{\partial x} + g (S - S_o) + v \frac{\partial v}{\partial x} + \frac{\partial v}{\partial t} = 0$$

$$-VT \frac{\partial h}{\partial x} + T \frac{\partial h}{\partial t} + A \frac{\partial v}{\partial x} = 0$$

into a pair of total differential equations solvable along two characteristic lines, C^+ , C^- drawn in the $x-t$ plane. In terms of Figure 3, these equations may be expressed as

$$\frac{dv}{dt} + \frac{g}{c} \frac{dh}{dt} + g (S - S_o) = 0$$

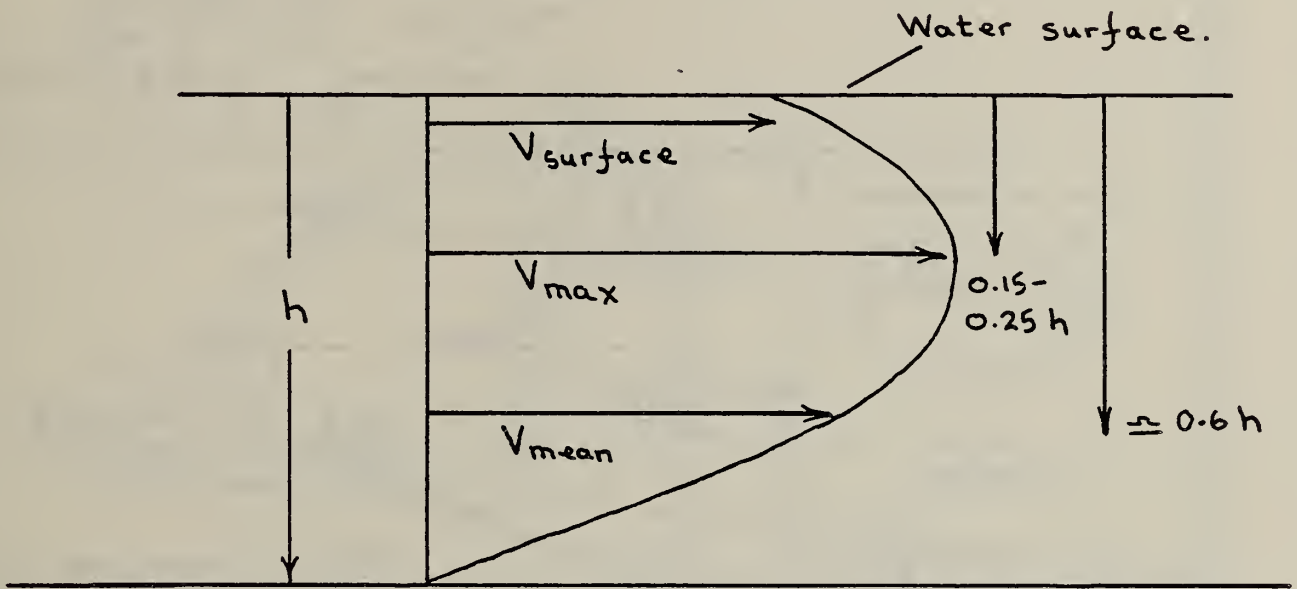


Figure 1. Typical velocity profile in open channel or partially filled pipe flow

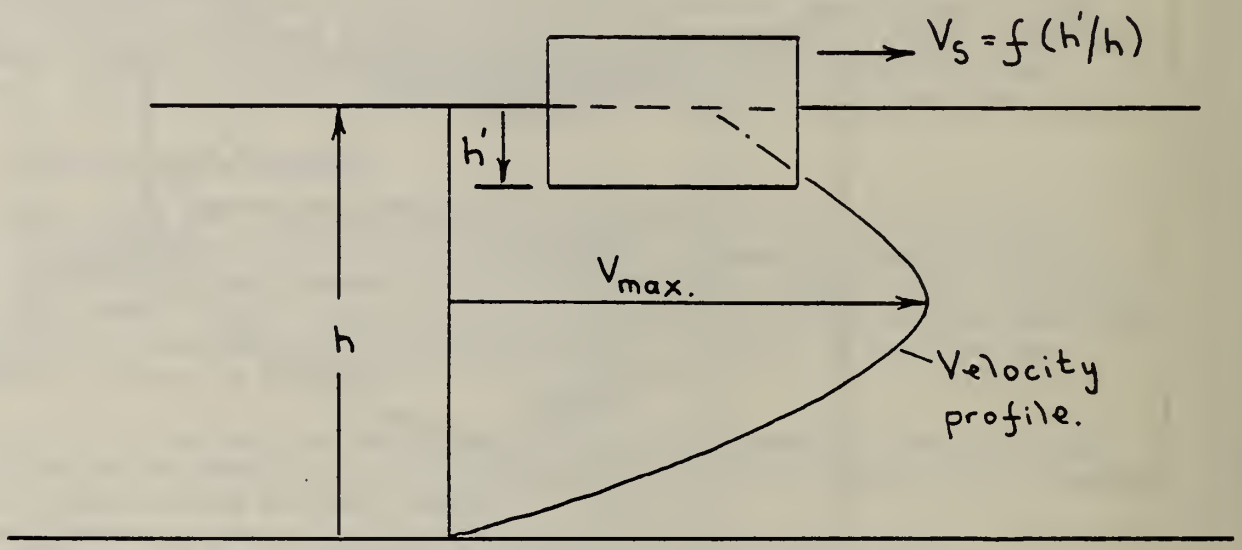


Figure 2. Floating solid velocity in open channel flow

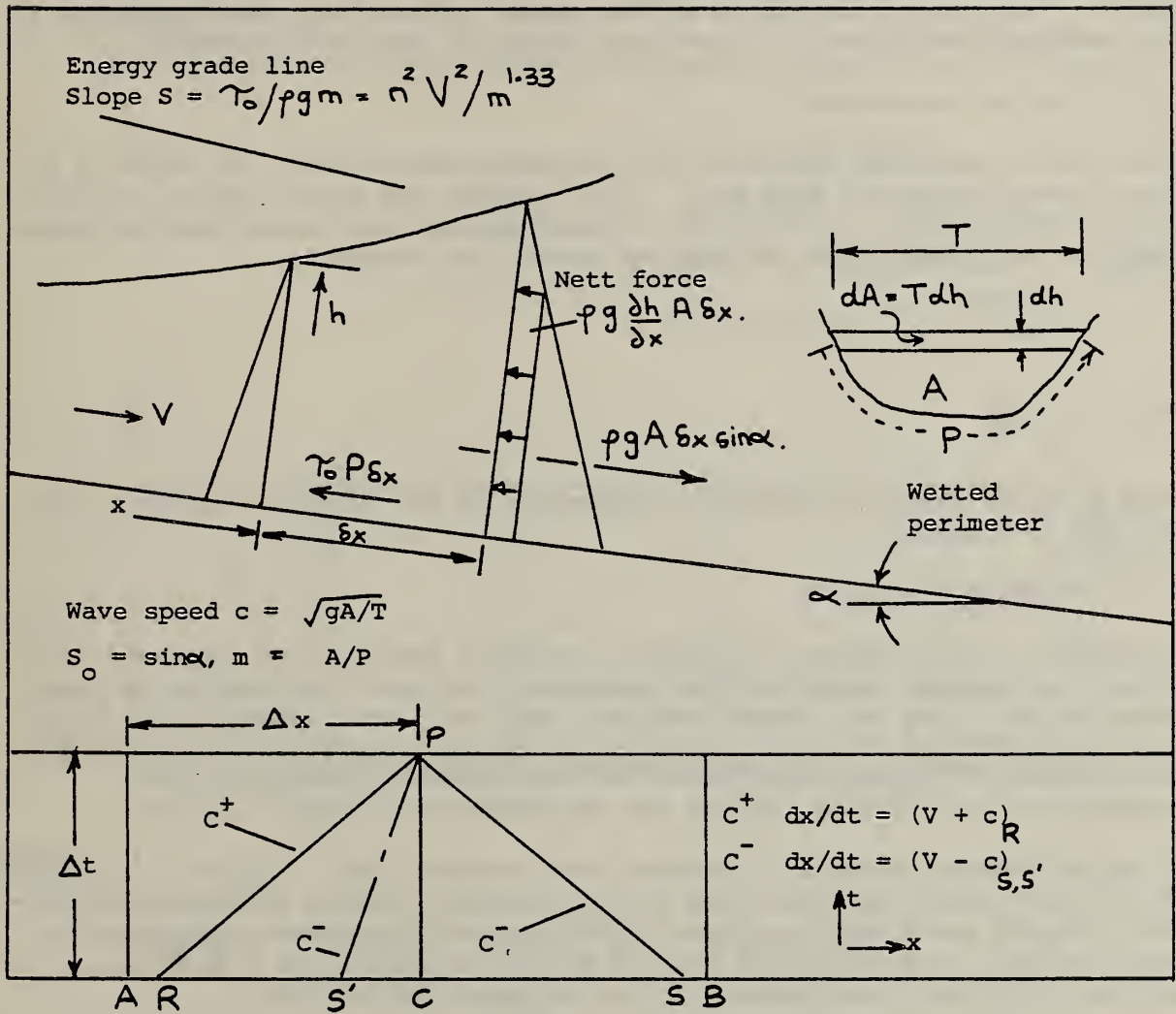


Figure 3. Summary of method of characteristics solution of the unsteady partially filled pipe flow equations

provided that $\frac{dx}{dt} = V \pm c$ where $c = \sqrt{\frac{gA}{T}}$

The slope of the characteristic lines in Figure 3 depends on both flow mean velocity, V , and local wave speed, c , and thus depend on the type of flow being considered. If $V < c$ then the flow is termed subcritical and disturbances traveling at wave speed may propagate both upstream and downstream. Conversely, if $V > c$, the flow is termed supercritical and disturbances can only propagate downstream. In the case of partially filled pipe flow in drainage sized pipes, normally of 100 mm diameter, and rarely set at slopes less than 1/100, it is supercritical flow that is the predominant design condition. The analysis presented in this paper, particularly with reference to pipe boundary conditions, is therefore limited to this flow condition.

2.3.1 Initial Conditions

The solution technique requires that flow depth and velocity are known at all nodes along the pipe at time zero. This requires the establishment of a small initial steady flow, (3) where the relevant depths, mean velocities and wave speed are calculated from the Manning steady flow equation:

$$Q = \frac{A}{n} m^{2/3} S_o^{1/2}$$

and $c = \sqrt{\frac{gA}{T}}$

where n is the surface roughness; a schematic of the solution technique is depicted in Figure 4.

2.3.2 Boundary Conditions

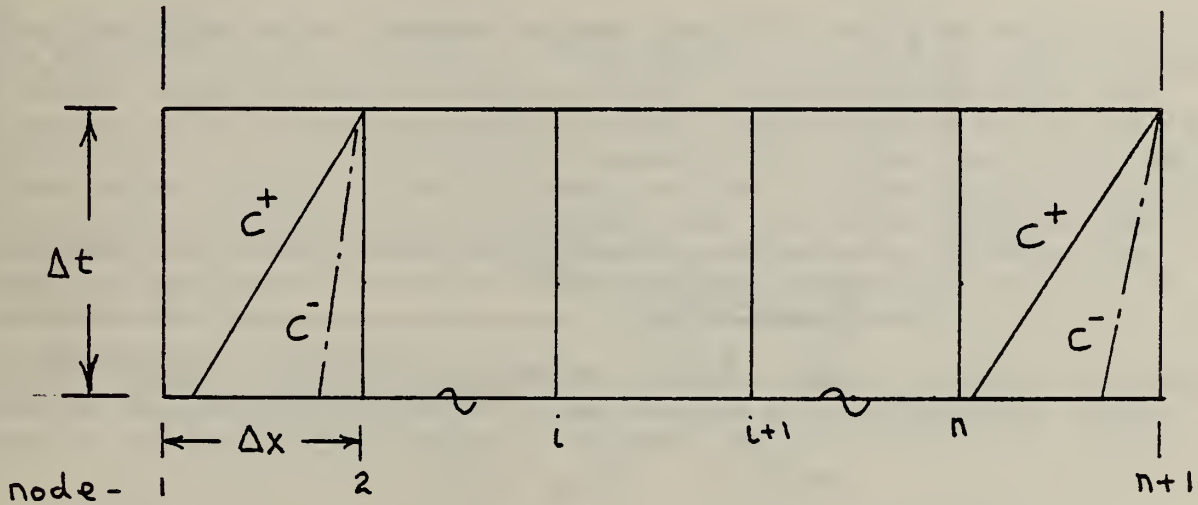
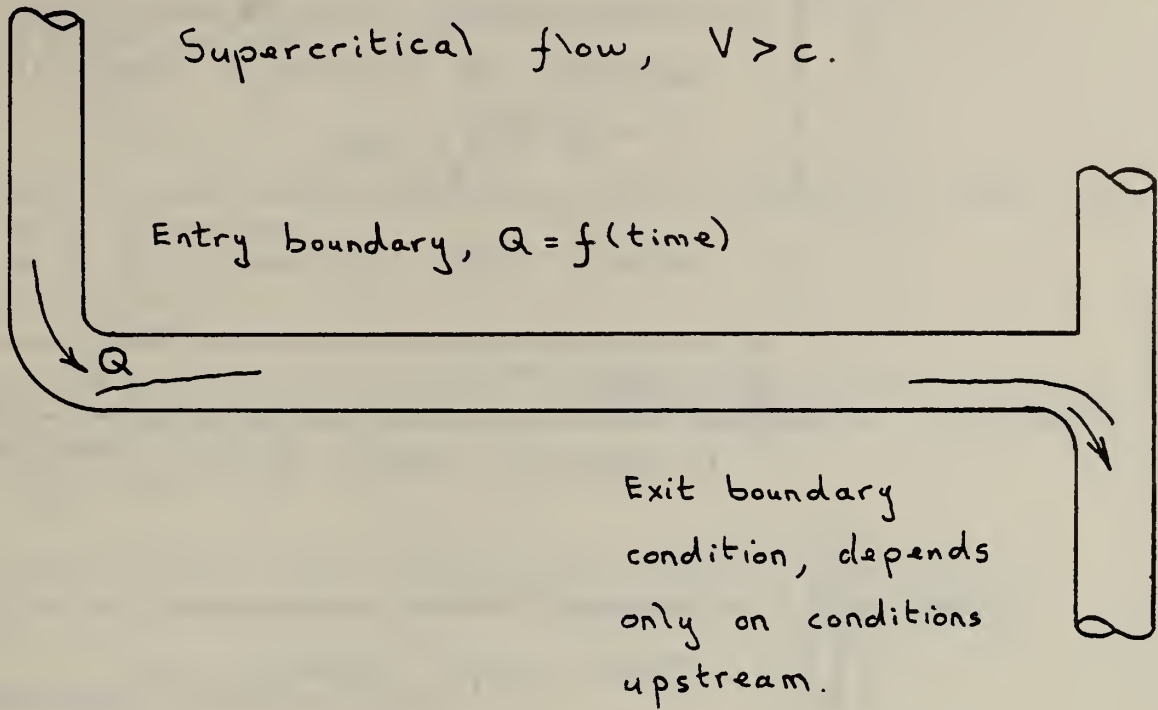
In addition to the initial conditions, mentioned above, it is necessary to define the boundary equations that determine flow depth or velocity at pipe inlet and exit. As the current analysis deals only with supercritical flow, the exit conditions are solely governed by the upstream flow conditions, i.e., the presence of the pipe exit cannot be communicated upstream as the approaching flow velocity exceeds the necessary wave speed.

The entry boundary condition requires more consideration. Figure 5 illustrates two boundary equations considered in this analysis, namely the simple assumption that the entry depth conforms to the "normal" flow depth appropriate to that flow rate, and calculated via the Manning equation, and a more realistic boundary condition incorporating the entry energy of the flow.

Referring to Figure 5, the entry energy of the flow may be determined in terms of the water jet velocity; u ,

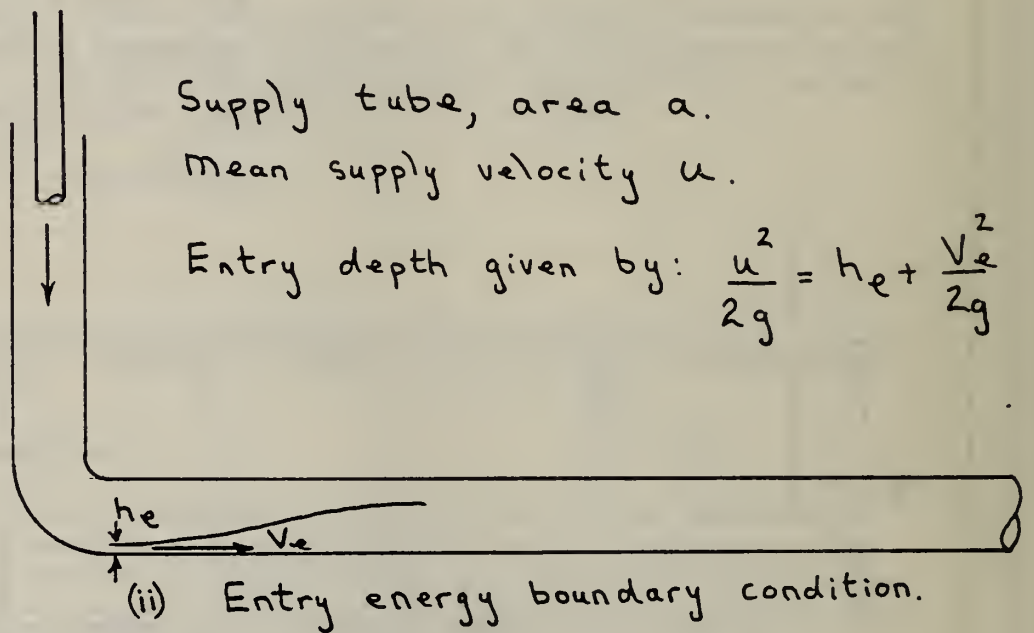
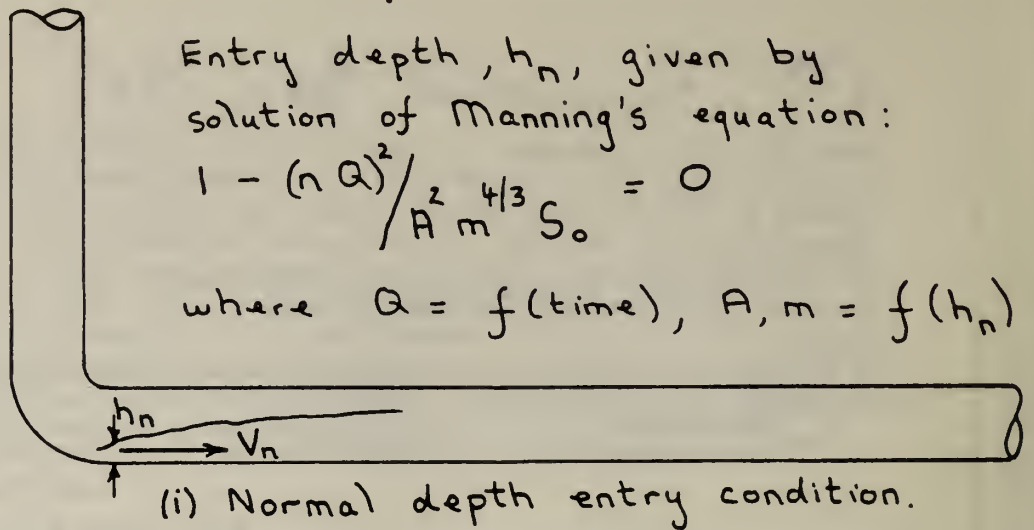
$$E = \frac{1}{2} \frac{u^2}{g} = \frac{Q^2}{2 g a^2}$$

where a , is the area of the delivering tube.



Note: initial conditions required at $t = 0$
at all nodes $1 - n+1$.

Figure 4. Schematic of the development of the solution in the x-t plane



Note: $h_e < h_n$
 $V_e > V_n$

Figure 5. Alternative entry boundary conditions

This entry energy is equated to the flow specific energy at entry to the partially filled pipe flow,

$$E = h + \frac{V^2}{2g}$$

where h and V are the flow depth and mean velocity at pipe entry as shown. By continuity it follows that:

$$E = h + \frac{Q^2}{2gA^2}$$

where A is the flow area, and a function of depth h . The inflow Q is known as a function of time and the flow depth may then be calculated by the expression:

$$h = \frac{Q^2}{2g} (1/a^2 - 1/A^2)$$

An iterative procedure is used, employing trial values to calculate A and satisfy the equivalence between entry and initial flow at entry specific energies.

2.4 CALCULATION OF SOLID VELOCITY

Figure 6 illustrates the effect on the solid if its floating velocity, V_s , is less than the mean flow velocity, V_1 . Relative to the carrying flow, the solid is seen to move back along the inflow profile, initially accelerating, but, depending on the velocity decrement, eventually passing behind the peak of the inflow profile and hence decelerating towards possible deposition in the "tail" of the inflow profile. It must be remembered that this description is based on solid velocity relative to the surrounding water, and while this migration is in process, the solid is being swept downstream at absolute velocities that depend on pipe gradient, diameter, pipe slope and the magnitude and shape of the inflow profile.

Figure 7 illustrates the calculation technique employed to determine the solid absolute velocity and its position along the pipe at any given time. At any time the solid velocity is assumed to be given by:

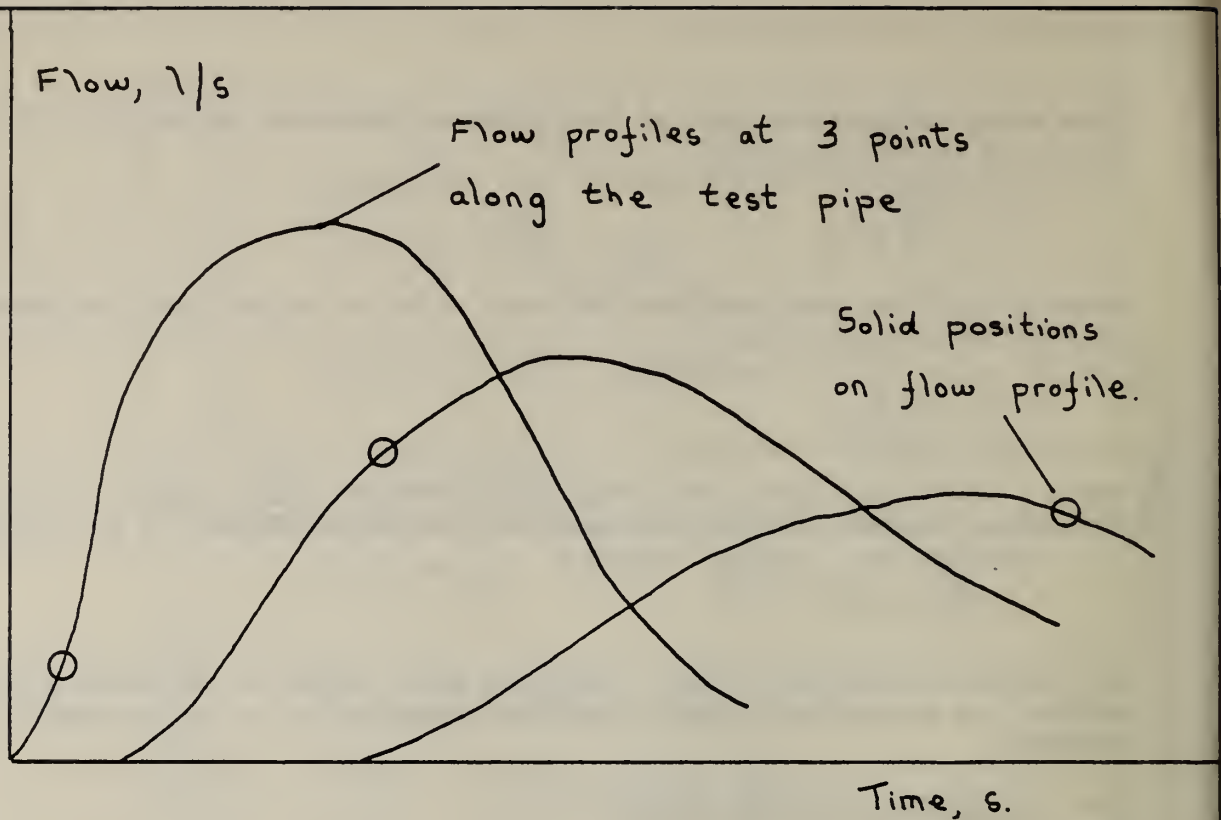
$$V_s = DV \cdot V_1,$$

where DV is <1 , the velocity ratio between the solid and the surrounding water defined as:

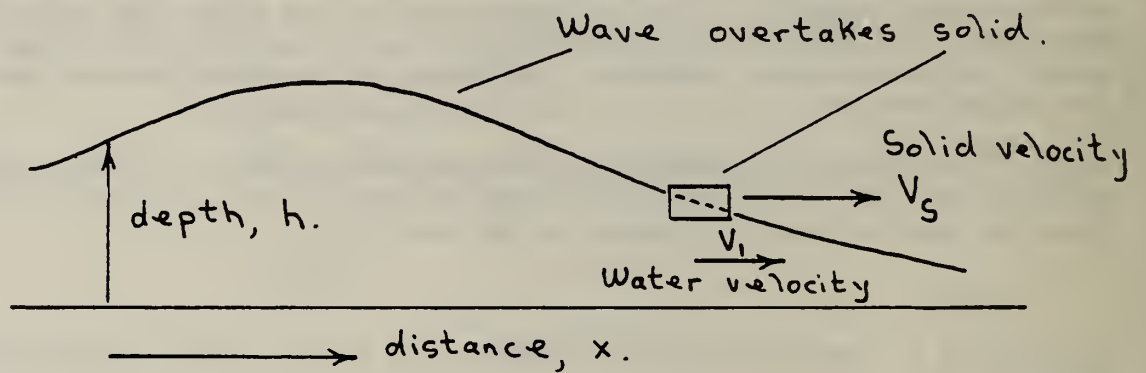
$$DV = \text{ratio of the solid velocity, } V_s, \text{ to the local mean water velocity, } V_1. \text{ Note that } V_1 \text{ is calculated by interpolation between nodes bracketing the solid position at any time.}$$

Once the V_s value is known, the solid position at the end of the next time step, $X_{t+dt} = X_t + V_s \cdot \Delta t$

and the process repeated at each subsequent time step.

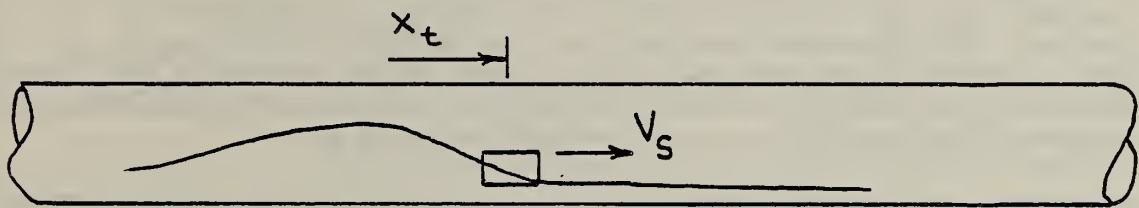
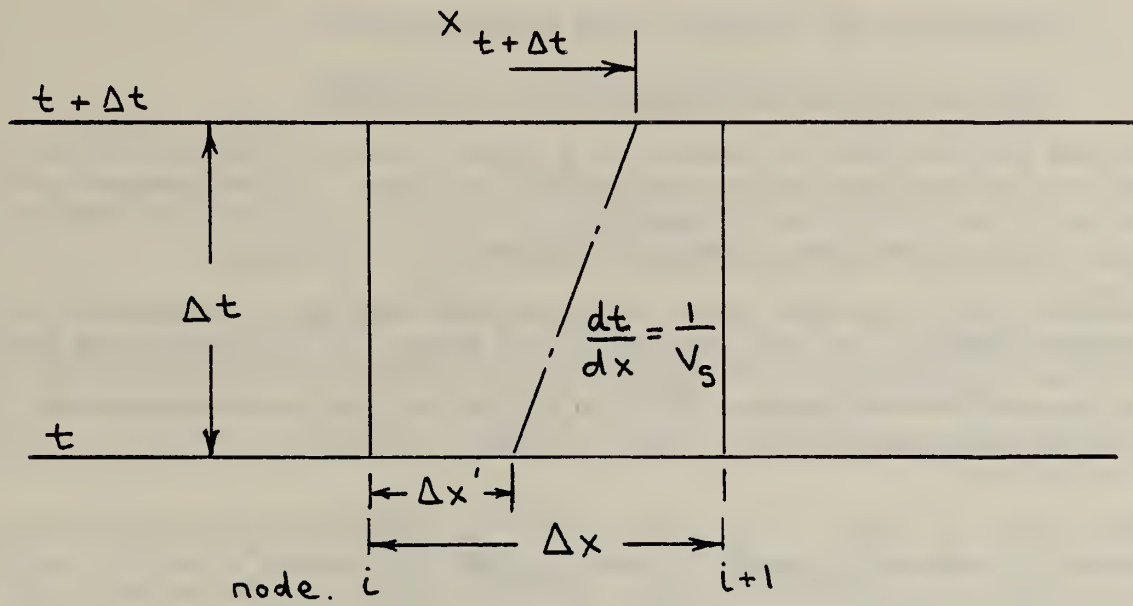


Note : as $V_s < V_i$, solid "moves back" along the flow profile.



Note : $V_s = DV \cdot V_i$, $DV < 1.0$

Figure 6. Solid migration through the inflow profile



$$V_s = DV. \left(V_i + \frac{\Delta x'}{\Delta x} (V_{i+1} - V_i) \right)$$

$$x_{t+\Delta t} = x_t + V_s \cdot \Delta t$$

Figure 7. Calculation of floating solid velocity and position in the pipe

3. DISCUSSION OF THE FLOATING SOLID TRANSPORT MODEL

3.1 STEADY FLOW SOLID TRANSPORT VELOCITY MEASUREMENT

Figure 8 illustrates the results of a primary study of transport of a typical NBS cylindrical model solid along a 1/150 gradient, 100 mm diameter test pipe at two steady water flow rates of 2.0 and 1.0 l/s. In each case the mean water flow velocity has been calculated from Manning's equation.

In the case of the empty solid it may be seen that the velocity ratio was roughly constant for both the steady flow rates. In these cases the solid floated at about its centre line. Some variations in the velocity ratio would be expected as the velocity profiles at the two flow depths would vary. However, the values are sufficiently close to support the use of a constant value in the simulation.

This would not appear to be the case for the solid when filled with water as a means of producing a specific gravity slightly in excess of unity. At 2 l/s the solid diameter and flow depth coincided almost exactly and the solid was observed to move steadily along the pipe with no disruption to the local water surface. However, at the 1 l/s flow rate the solid was uncovered in the flow, resulting in the flow disruption shown and a much lower transport velocity. It may be concluded from these results that the assumption of a constant ratio between floating solid and accompanying water velocity is only acceptable above certain limiting flow rates, sufficient to provide adequate depths of flow. In the case of the empty solid flow depths less than 18 mm would result in the same effect, i.e. flow rates, at 1/150 gradient, of approximately 0.4 l/s. In the full solid case the limiting flow rate would be in the region of 2 l/s. In both cases the flow disruption at flow rates below the values mentioned would be expected to result in deviations between measured solid velocities and the output of a simulation based on constant velocity ratios.

Measurement of similar velocity ratios at various gradients and flow rates is currently part of the NBS research programme in conjunction with work at Brunel. For the simulation presented in this paper the velocity ratios are assumed to apply at all pipe gradients, however, as flow depth is dependent on gradient, the limiting flow rates mentioned will also be dependent on gradient. For example, the 18 mm depth limit for the empty solid will be reached at a flow rate of 0.75 l/s at a 1/80 gradient and 1.1 l/s at 1/40. In view of these limits, it might be expected that the model, as presented, will perform best at the flatter pipe gradients.

3.2 EXPERIMENTAL VERIFICATION

Figure 9 illustrates the test pipe configuration employed to record the transport performance of NBS cylindrical solids in June 1980. These results have been utilized in the current paper to provide experimental data as a comparison to the output of the simulation described.

The test pipe consisted of 14 m of 100 mm diameter clear UPVC pipe, Manning coefficient 0.008, capable of gradient adjustment from 1/40 to 1/300. Solid

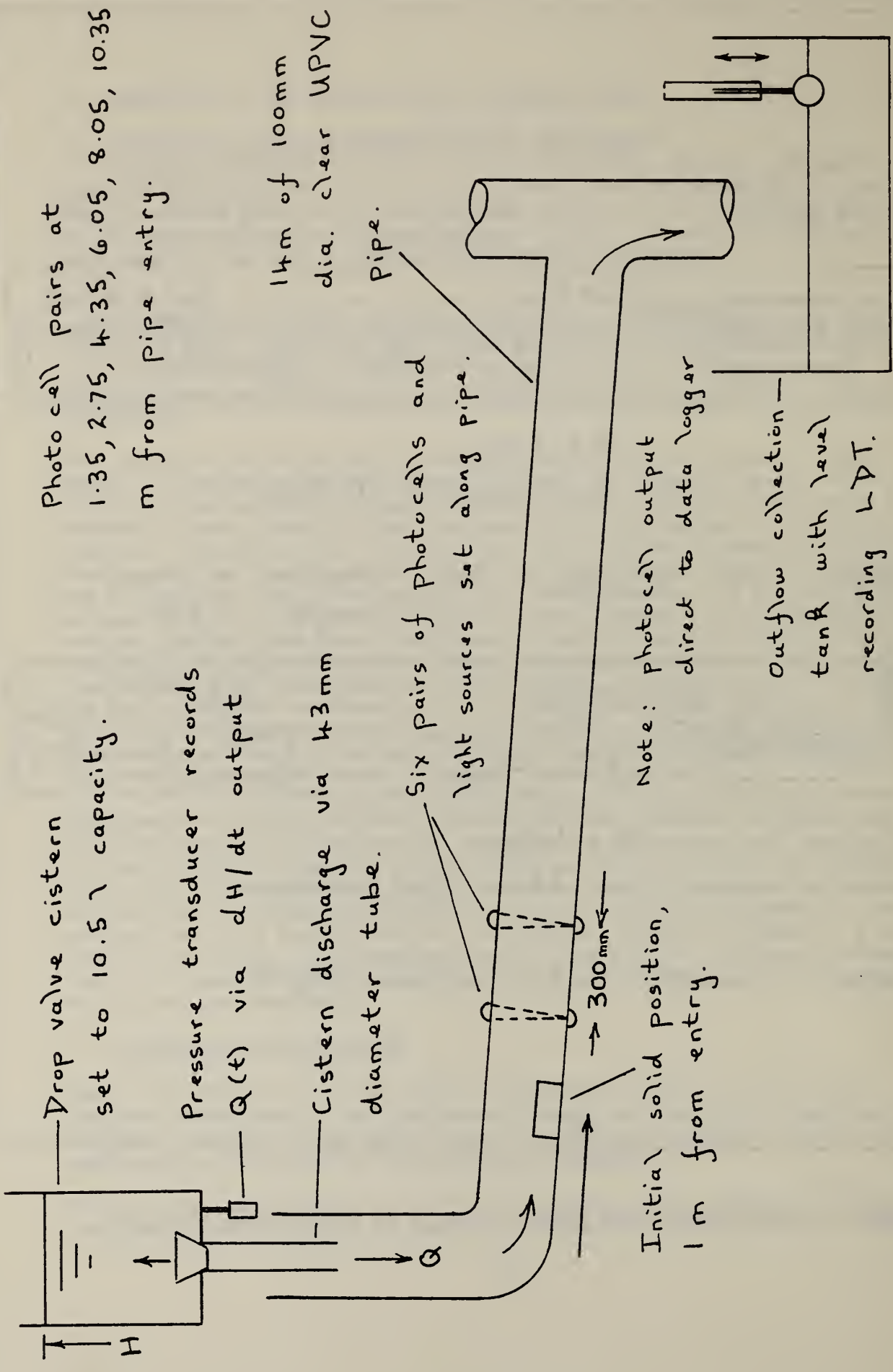


Photo cell pairs at
1.35, 2.75, 4.35, 6.05, 8.05, 10.35
m from pipe entry.

Figure 9. Schematic of solid transport test rig

velocity was recorded by six pairs of photoelectric cells at 0.3 m separation along the first 12 m of pipe. Output from the photocells was fed directly to a microcomputer used produce the data illustrated in Figure 10.

The volume of water leaving the pipe ahead of the solid was recorded by means of level sensing in the terminal collection tank.

The solids tested were initially placed in the test pipe and inflow to the pipe was provided by a Geberit drop valve cistern, set to 10.5 liter capacity, and supplying water to the test pipe via a 43 mm diameter downpipe as shown. Discharge rates from the cistern were monitored by means of a pressure transducer and a high speed pen recorder and provided the input data for the current simulation. The solid used in all tests considered in this report was an NBS hollow cylindrical model solid, length 80 mm, 37 mm diameter, initially stationary in the pipe 1 m from entry.

3.3 ENTRY BOUNDARY CONDITIONS AND UNSTEADY FLOW SOLID TRANSPORT

Figures 11, 12 and 13 illustrate the predicted solid velocities along 14 m of 100 mm diameter pipe following a 10.5 l discharge into the system, the peak inflow being 6 l/s and the inflow duration being less than three seconds. Two model boundary conditions are illustrated: namely normal depth at entry and the dependence of the entry depth on flow energy. A velocity ratio of 0.9 was used to illustrate the following effects of the boundary condition choice on the predicted solid velocity.

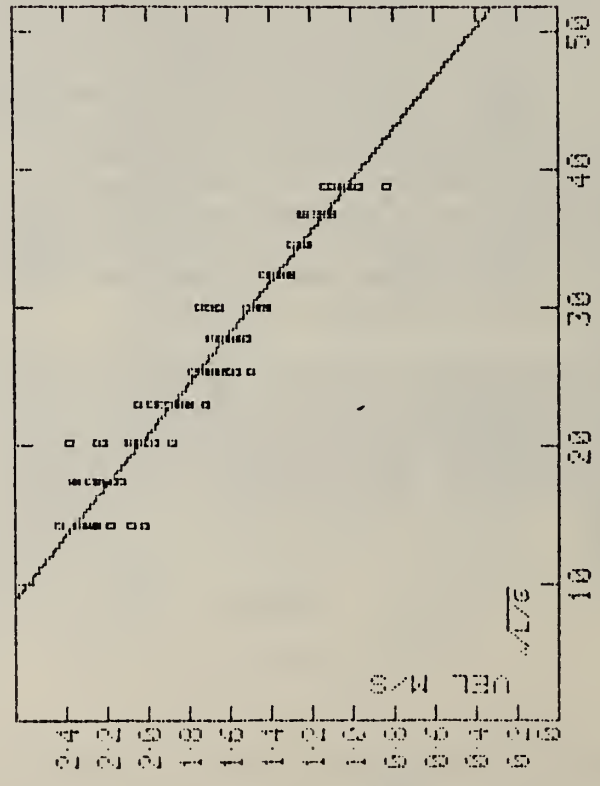
- (i) Normal depth at entry dictates that the maximum flow depth occurs at this point as the inflow profile peaks. Thereafter the depth decreases along the whole pipe length. This condition also limits the velocity at entry to that calculated from Manning's equation.
- (ii) Normal depth is dependent on pipe gradient so that the entry depth and velocity depend on pipe gradient. However, as the cases chosen are restricted to supercritical flow, and as an air gap exists between the cistern discharge pipe and the test drainage pipework, the entry conditions would be expected to remain constant and independent of gradient. Figure 14 illustrates the predicted flow depths and velocities at the pipe entry for both the entry energy and normal depth models. It will be seen that the energy model predictions are unaffected by pipe gradient. Further, it will be seen that entry depth decreases with increasing flow rate in the energy model, as the kinetic energy term predominates, the opposite to the normal depth model where flow depth and velocity vary together through Manning's equation.

Comparison of the predicted solid velocity results indicate that the normal depth assumptions are incapable of providing solid velocities of the same magnitude as those observed on the test rig and included in Figures 11 to 13. The assumption that the entry conditions are dependent on the inflow energy, however, give solid velocities close to those recorded; i.e. agreement better than 10 percent at pipe entry.

NBS RESEARCH PROGRAMME - BRUNEL UNIVERSITY
DR JA SWAFFIELD & BST MARRIOTT

14.2 METRES, 100 MM UPVC PIPE
- WC. WITH FLUSH VALVE TYPE CISTERN.
FLUSH VOLUME = 10.5 LITRES.
DATE 14/6/80

GRADIENT 1 IN 150
80 MM LONG 37 MM DTA EMPTY SOLID.
GRADIENT 1 IN 150



$V = 3.1346 - .0545(\text{SQR}(L/G))$

$U = 0, \text{SQR}(L/G) = 57.5$

CORRELATION COEFFICIENT (CC) = -.9614
CC ↑ 2 * 100 = 92.4%

NBS RESEARCH PROGRAMME - BRUNEL UNIVERSITY
DR JA SWAFFIELD & BST MARRIOTT

14.2 METRES, 100 MM UPVC PIPE
- WC. WITH FLUSH VALVE TYPE CISTERN.
FLUSH VOLUME = 10.5 LITRES.
DATE 14/6/80

GRADIENT 1 IN 150
80 MM LONG 37 MM DTA EMPTY SOLID.
GRADIENT 1 IN 150

RUN NO.	Z FLUSH AHEAD	STOP POSTN.	POINT VELOCITY METRES FROM WC. SENSOR SEPARATION.	1	2	3	4	5	VELOCITY, M/S
14.01	7.1	FREE	2.242	2.208	1.777	1.479	1.479	1.254	1.076
14.02	1.2	FREE	3.425	1.999	1.644	1.479	1.479	1.243	1.076
14.03	4.5	FREE	3.259	2.243	1.527	1.491	1.491	1.208	1.088
14.04	3.3	FREE	3.176	2.049	1.700	1.516	1.516	1.075	1.075
14.05	1.0	FREE	3.084	2.267	1.710	1.710	1.710	1.073	1.073
14.06	1.1	FREE	3.340	2.041	1.526	1.749	1.749	1.017	1.017
14.07	1.1	FREE	3.312	2.041	1.526	1.409	1.409	1.089	1.089
14.08	1.1	FREE	3.348	1.873	1.491	1.465	1.465	1.084	1.084
14.09	1.4	FREE	3.013	1.866	1.491	1.465	1.465	1.084	1.084
14.10	0.9	FREE	3.242	2.099	1.487	1.444	1.444	1.259	1.077

ST.	MEAN	DEV.	MAX.	MIN.
	1.9	0.00	2.243	2.088
	1.4	0.00	3.425	0.146
	0.9	0.00	2.013	1.777
			1.873	1.487

Figure 10: Typical Solid Transport Data as Produced by the Apple II System.

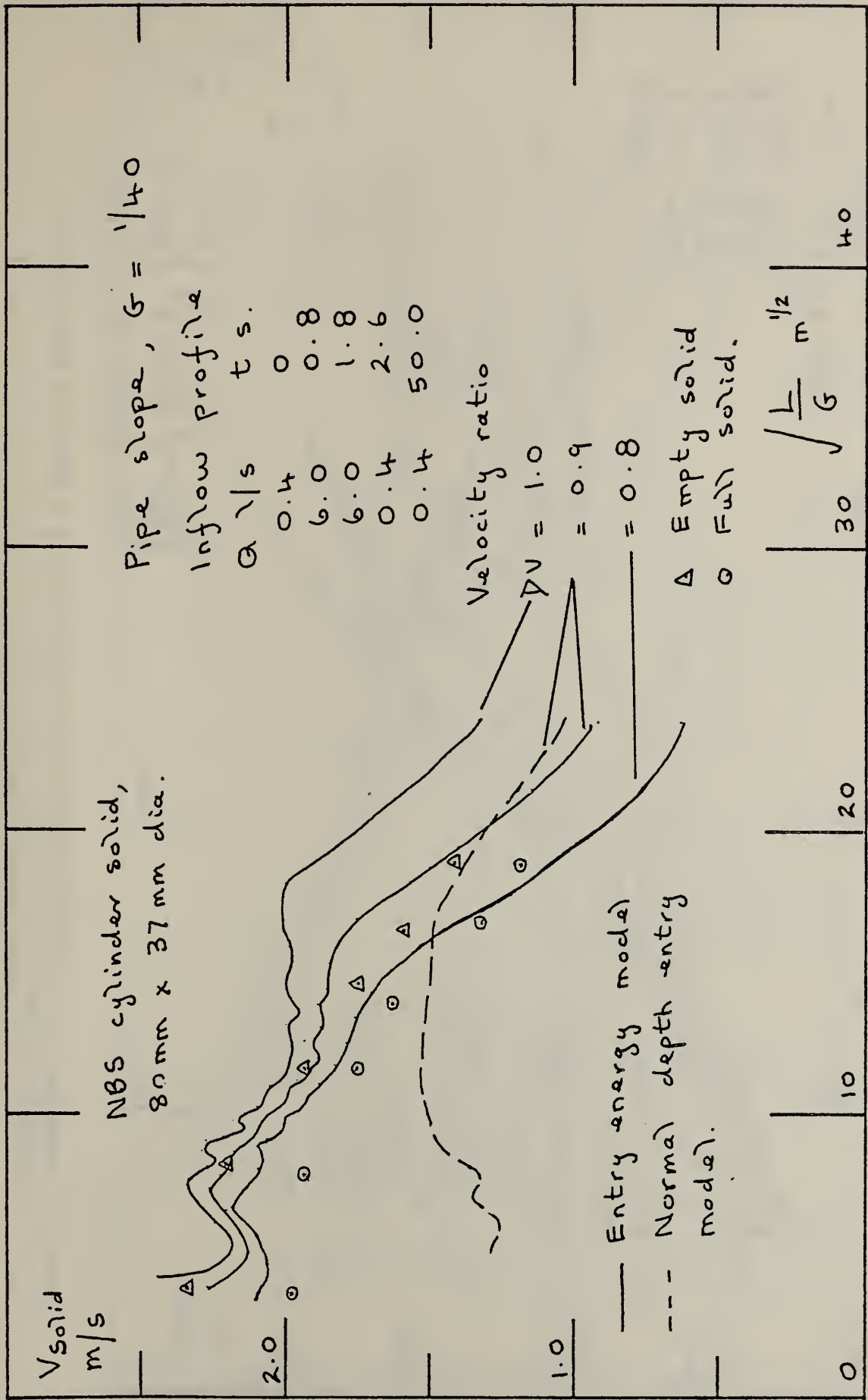


Figure 11: Comparison of Observed and Predicted Solid Velocities Along the Test Pipe at a Gradient of 1/40.

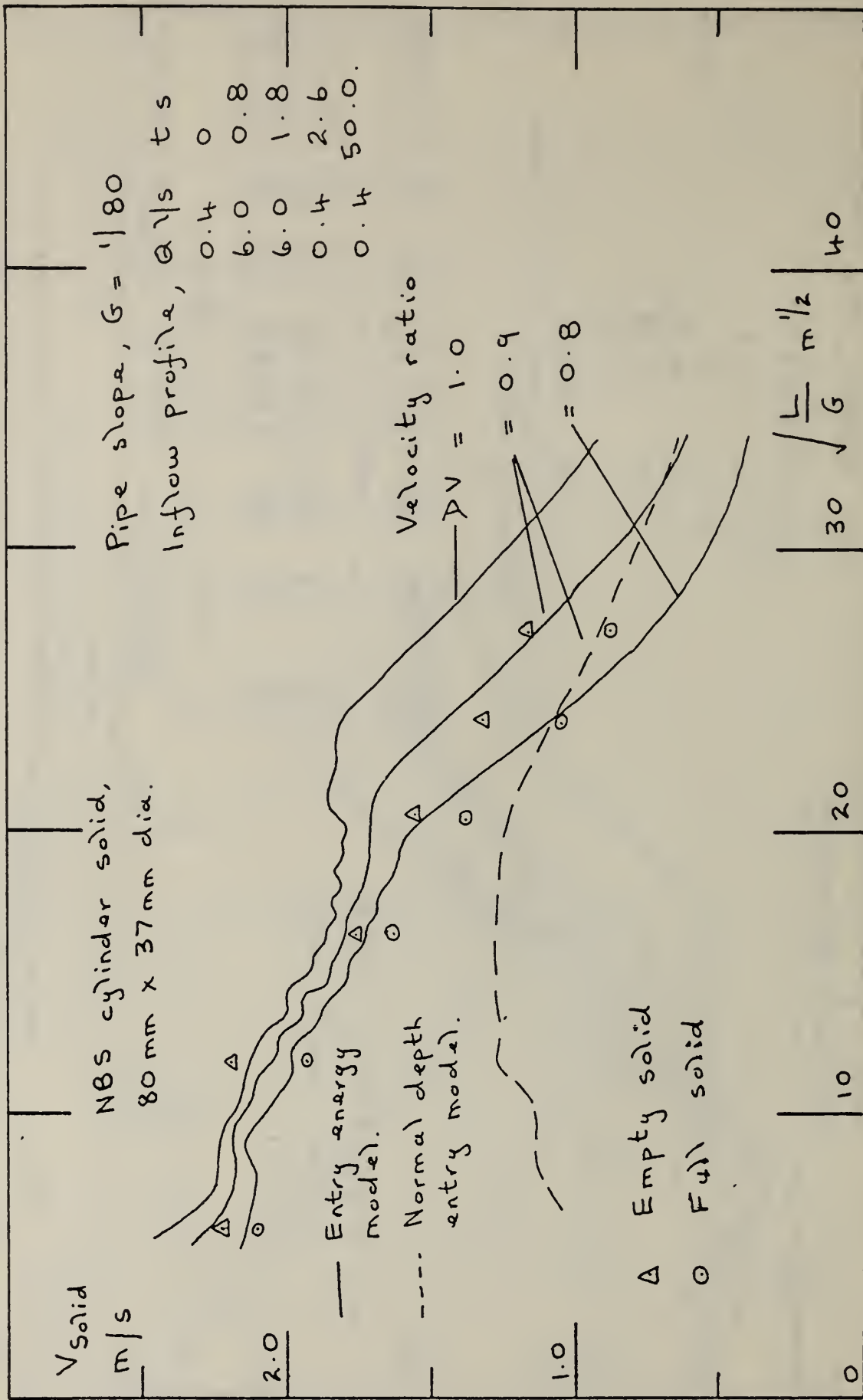


Figure 12: Comparison of the Observed and Predicted Solid Velocities Along the Test Pipe at a Gradient of 1/80.

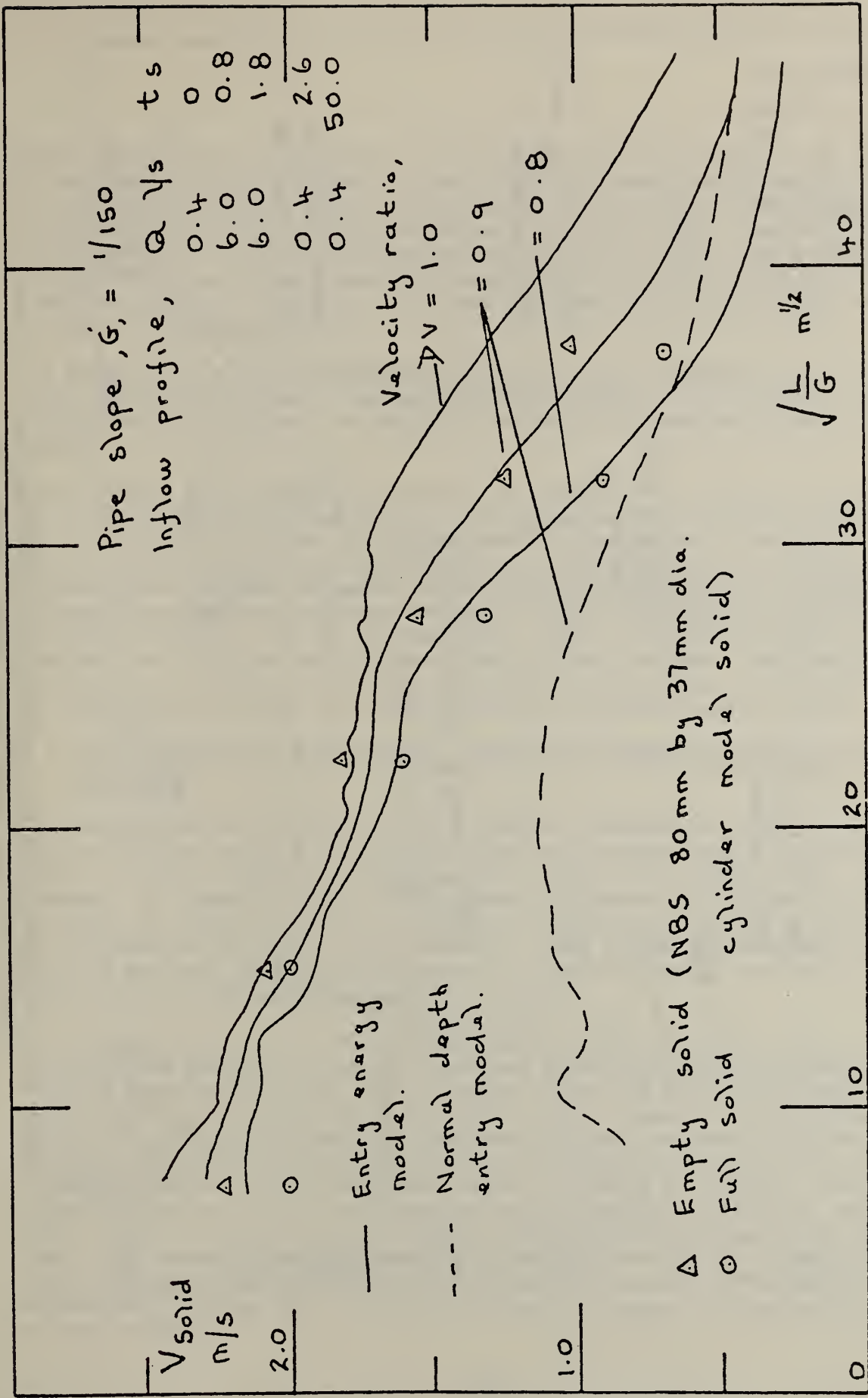


Figure 13: Comparison of the Observed and Predicted Solid Velocities Along the Test Pipe at a Gradient of 1/150.

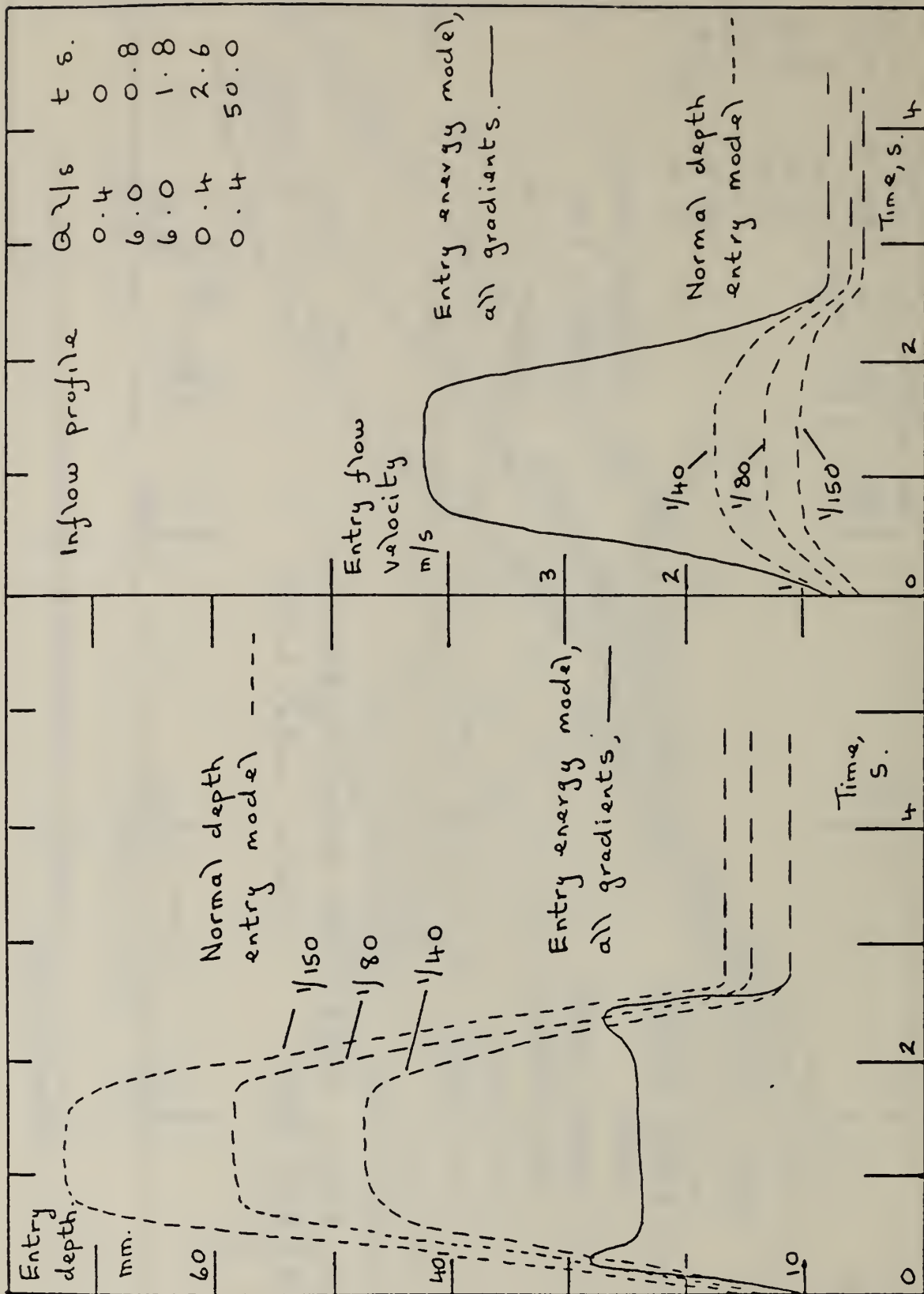


Figure 14: Comparison of the Flow Velocity and Depth Predictions at Pipe Entry for the Normal Depth and Inflow Energy Boundary Conditions.

Figure 15 illustrates the effect on flow depth along the pipe for the two types of boundary conditions above. As mentioned, the normal depth condition results in a gradually reducing maximum depth along the whole pipe, indicating a progressive attenuation along the system. The energy model however, indicates a maximum depth point reached between 5-7 m from pipe entry, the exact location moving downstream with increasing flowrate. This is effectively the transition zone from the entry energy to the normal flow depth modified slightly by an overlying attenuation effect.

For each of the 3 gradients shown (1/40 1/80, 1/150) maximum depth is slightly less than the normal depth appropriate to the maximum inflow of 6 l/s, the divergence being greatest, as expected, in the 1/150 case and least in the 1/40 case.

These results are considered sufficient to show that the energy entry condition is the more realistic model for the flow conditions that existed in the experiments. It also indicates that the method of characteristics solution is capable of dealing with transition phenomena under unsteady flow conditions. This observation is limited to supercritical flow at present due to the possibility of hydraulic jump formation in subcritical flows set up under the conditions described, however, this is not considered a major limitation as pipe gradients flatter than 1/150 are rare in most practical applications. The subcritical case will be the subject of further investigations as Brunel experimental data is available for the NBS cylindrical solid at gradients down to 1/300.

3.4 FLOATING SOLID TO FLOW VELOCITY RATIO AND ITS EFFECT ON PREDICTED SOLID TRANSPORT

The steady flow test results at 1/150 gradient discussed in section 3.1 indicated that the assumption of a constant velocity ratio between solid and accompanying flow, even for a nominally floating solid, broke down in shallow flow conditions. Reference to Figure 13, for 1/150 gradient, indicates that in this case, close agreement was achieved between the measured and predicted solid velocities over the majority of the pipe length, however a study of the depth versus time profiles for this simulation indicates that the flow depths were sufficient to comply with the restrictions identified earlier.

As might be expected, with steepening gradient, this is not the case at the 1/80 and 1/40 gradients, thus the predicted solid velocities in these two cases would be expected to exceed those recorded during the tests. Due to the reduced depth characteristic of the steeper pipe gradients, the effective blockage of the solid within the pipe flow cross section increases which produces a secondary "blocking" effect, identifiable in Figures 11 and 12. The increased blockage tends to 'store' more water behind the solid in practice than predicted by the simulation, which assumes zero disruption to the flow around the solid. Hence in the later pipe length stage, the solid transport velocity will tend to be higher in practice than the value predicted by the simulation. This effect is clearly seen for both the 1/40 and 1/80 cases, of Figures 11 or 12 particularly for the 'full' solid, which has the larger flow disruption effect as seen in Figure 8.

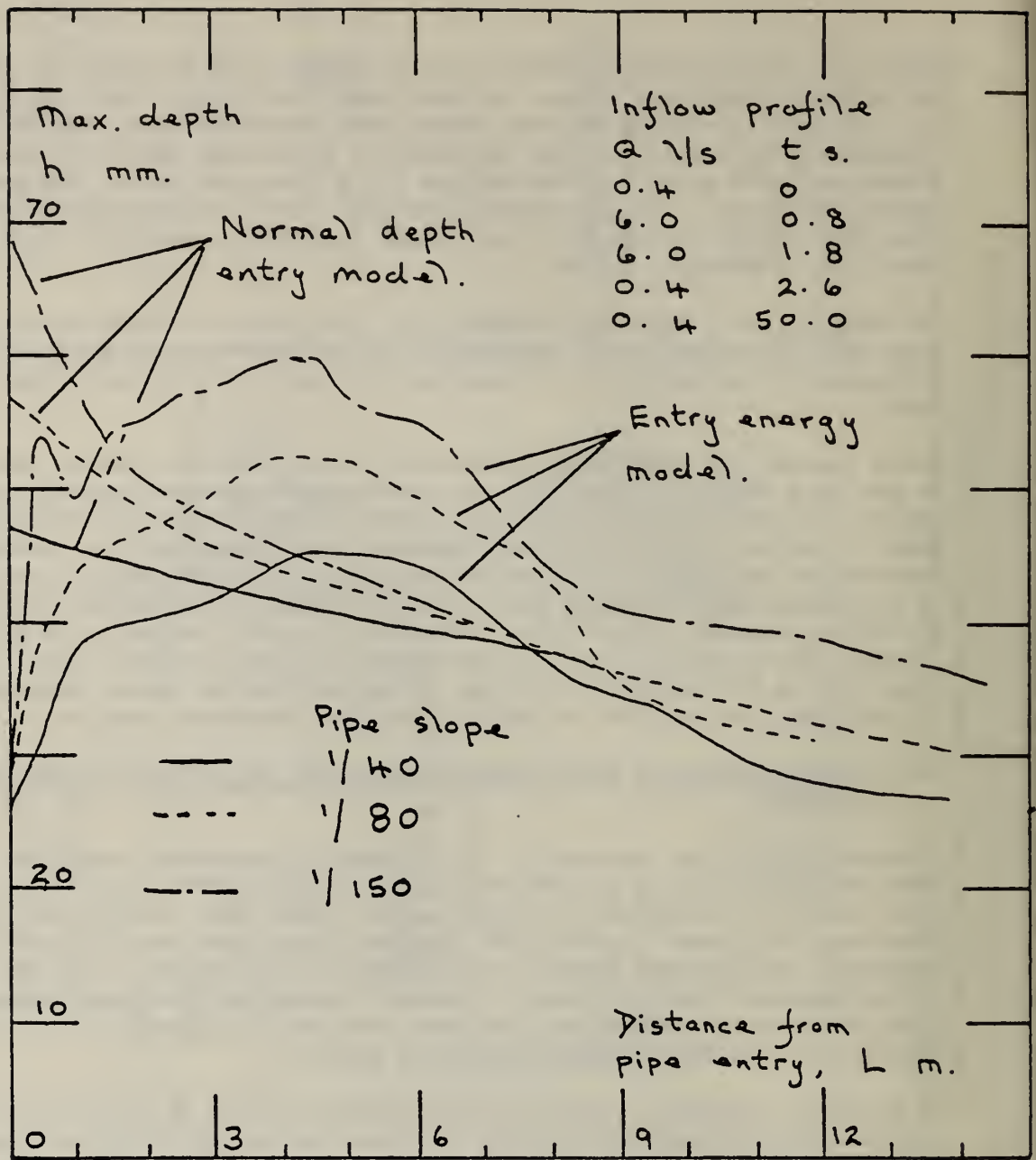


Figure 15: Maximum Predicted Depths Along the Test Pipe for both Normal Flow Depth and Entry Energy Upstream Boundary Conditions.

While Figures 11 to 13 illustrate the variations in solid velocity along the waste pipe, it will be noted that the total transport time increases with reductions in both pipe gradient, from 1/40 to 1/150, and solid velocity ratio, from 1.0 to 0.8. Table 1 contains predicted results for a 14 m pipelength and reinforces the 'backward' movement of a solid through the inflow profile illustrated in Figure 6. Table 1 was compiled for the constant inflow profile illustrated in Figure 11. This relative motion of the solid through the inflow profile is also dependent on the initial position of the solid in the profile. Figure 16 illustrates, for a velocity ratio of 0.8, the effect of introducing the solid at various times during the inflow duration. These results indicate that solid transport efficiency is severely reduced by late insertion. The results are significant for WC design, particularly in water conservation and reduced flush volume designs.

Table 1. Predicted Total Solid Transport Time for A 14 m Pipe for a Range of Gradients and Velocity Ratios

	Time to reach pipe discharge, secs.			
	Gradient	1/40	1/80	1/150
Velocity Ratio	1.0	8.50	10.20	12.08
	0.9	10.48	13.40	16.80
	0.8	13.78	17.80	24.68

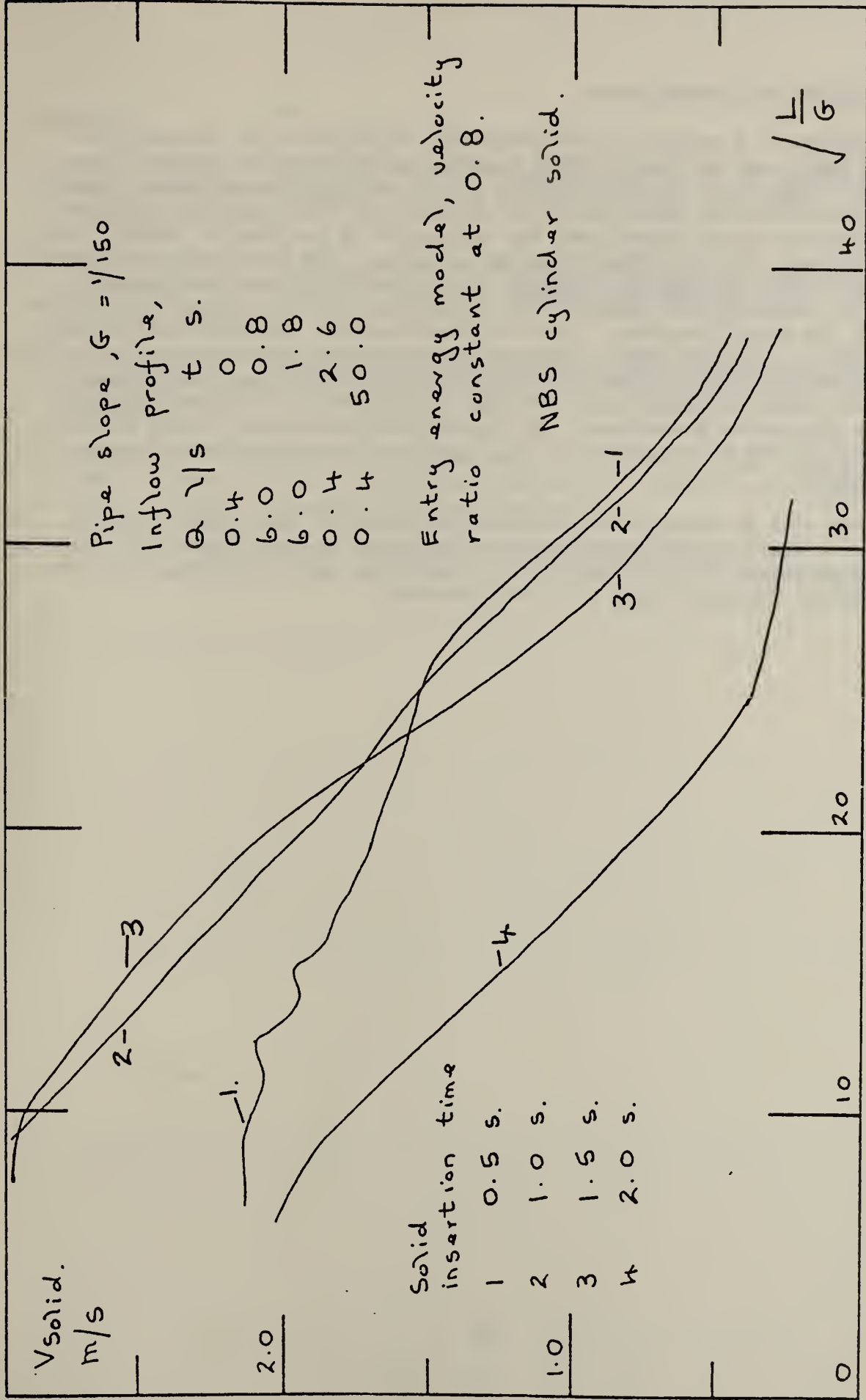


Figure 16: Illustration of the Effect of Solid Insertion Time on Predicted Transport Along the Test Pipe.

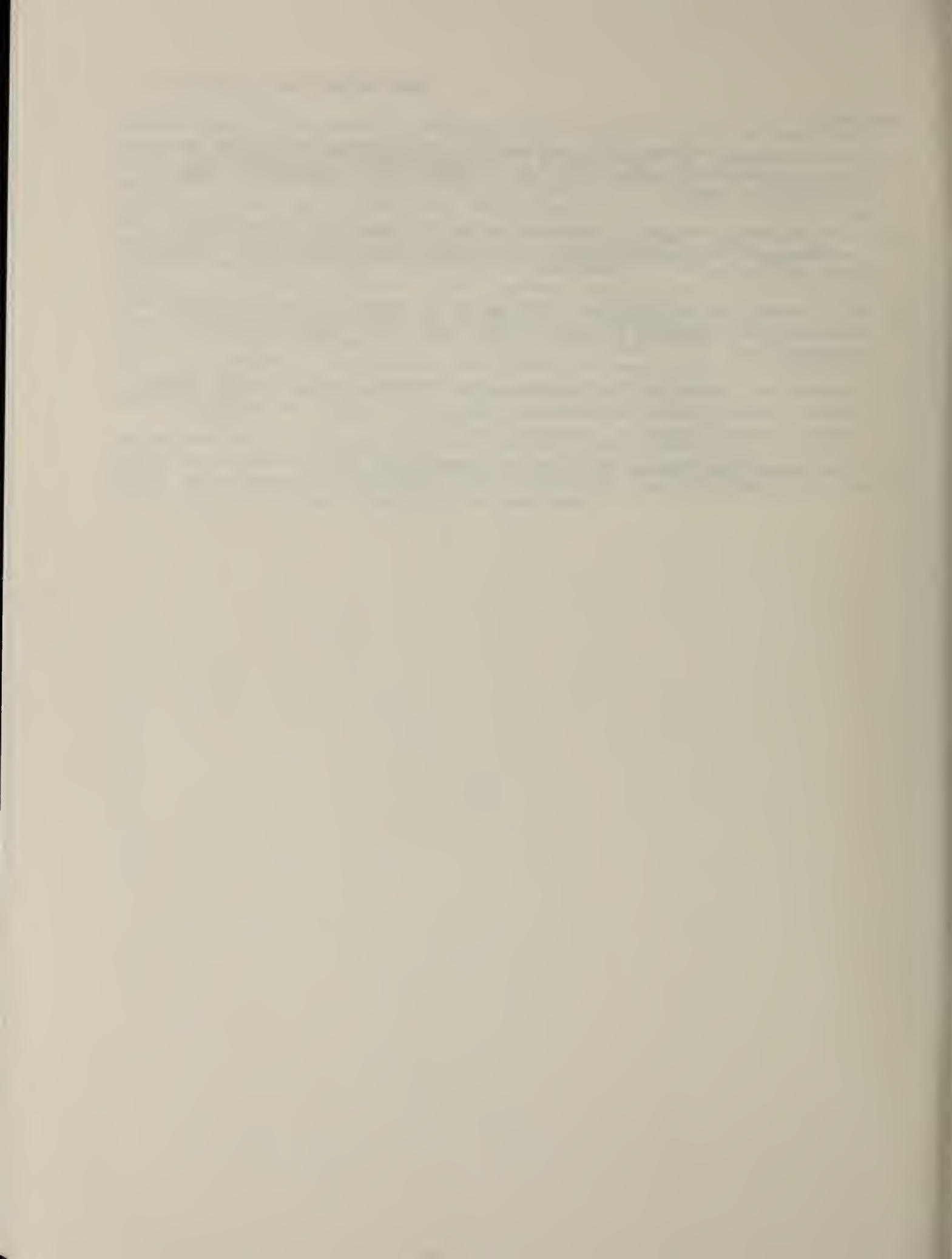
4. CONCLUSIONS AND FURTHER WORK

The application of a method of characteristics solution to the unsteady flow equations describing partially filled pipeflow in the special case of floating solids with known solid to flow velocity ratios has been demonstrated. Experimental verification has indicated that, provided the flow depth is sufficient to give flotation and provided that the disruption to the flow is slight, accurate predictions of solid velocity may be achieved. The study has also shown that the inclusion of flow entry energy as an alternative upstream boundary condition in supercritical channel flow is practical and is responsible for the success of the model presented. This upstream boundary condition will be utilized further in parallel work at Brunel concerned with flow attenuation prediction. The method is also shown to be capable of predicting the transition to normal flow depth, including the overlying attenuation of the flow depth profile as it progresses downstream. The results are considered to have particular application for water conserving w.c. application with existing drainage pipe networks.

Further work will be required to determine the solid to water mean velocity ratios and to identify the dependence of such ratios on pipe slope and flow depth. An extension of the model to the subcritical case, including provision for a potential hydraulic jump will be considered.

REFERENCES

1. J. A. Swaffield "An Initial Study of the Application of the Method of Characteristics to Unsteady Flow in Partially Filled Pipe Flow". NBSIR 81-2308, July 1981.
2. J. A. Swaffield "Application of the Method of Characteristics to Model the Transport of Discrete Solids in Partially Filled Pipe Flow". BSS 139, February 1982.
3. J. A. Swaffield "Application of the Method of Characteristics to Predict Attenuation in Unsteady Partially Filled Pipe Flow." NBSIR 82-2478, December 1981.
4. P. Burberry "Techniques for the Estimation of Flows in Foul Drains in the Light of Present Water Conservation Proposals". Seminar on Drainage Design, Brunel University, Uxbridge, May 1978.
5. V. T. Chow "Open Channel Hydraulics", McGraw Hill, 1970.



U.S. DEPT. OF COMM. BIBLIOGRAPHIC DATA SHEET (See instructions)		1. PUBLICATION OR REPORT NO. 82-2614	2. Performing Organ. Report No.	3. Publication Date
4. TITLE AND SUBTITLE The Prediction of Floating Solid Velocities in Unsteady Partially Filled Pipe Flow				
5. AUTHOR(S) John A. Swaffield				
6. PERFORMING ORGANIZATION (If joint or other than NBS, see instructions) NATIONAL BUREAU OF STANDARDS DEPARTMENT OF COMMERCE WASHINGTON, D.C. 20234			7. Contract/Grant No.	8. Type of Report & Period Covered
9. SPONSORING ORGANIZATION NAME AND COMPLETE ADDRESS (Street, City, State, ZIP) Department of Housing and Urban Development 451 7th Street, SW Washington, D.C. 20410				
10. SUPPLEMENTARY NOTES <input type="checkbox"/> Document describes a computer program; SF-185, FIPS Software Summary, is attached.				
11. ABSTRACT (A 200-word or less factual summary of most significant information. If document includes a significant bibliography or literature survey, mention it here) The method of characteristics is applied to solve the unsteady partially filled pipe flow equations and to predict the velocity of floating solids assumed to travel at a fixed percentage of the local flow velocity. Experimental verification for the technique is provided for cylindrical solids in 100 mm diameter drainage pipe at a range of gradients from 1/40 to 1/150. The system upstream boundary conditions are shown to be capable of representation in terms of the inflow energy at the pipe entry section. Steady flow floating solid to flow velocity ratios are presented at 1/150 pipe gradient and further areas of experimental work to determine the variation of these ratios with pipe gradient and flow depth are identified.				
12. KEY WORDS (Six to twelve entries; alphabetical order; capitalize only proper names; and separate key words by semicolons) floating solids; partially filled pipe flows; pipe flow with solids; plumbing drains.				
13. AVAILABILITY <input checked="" type="checkbox"/> Unlimited <input type="checkbox"/> For Official Distribution. Do Not Release to NTIS <input type="checkbox"/> Order From Superintendent of Documents, U.S. Government Printing Office, Washington, D.C. 20402. <input checked="" type="checkbox"/> Order From National Technical Information Service (NTIS), Springfield, VA. 22161			14. NO. OF PRINTED PAGES	
			15. Price	

